



TITLE:

# Studies on the Fluorine Generation by Fused Salt Electrolysis of KF·2HF at about 100°C

AUTHOR(S):

YOSHIZAWA, Shiro; WATANABE, Nobuatu; ISHII,  
Masahito

---

CITATION:

YOSHIZAWA, Shiro ...[et al]. Studies on the Fluorine Generation by Fused Salt Electrolysis of KF·2HF at about 100°C.  
Memoirs of the Faculty of Engineering, Kyoto University 1960, 22(4): 422-439

ISSUE DATE:

1960-10-31

URL:

<http://hdl.handle.net/2433/280482>

RIGHT:

## Studies on the Fluorine Generation by Fused Salt Electrolysis of $\text{KF}\cdot 2\text{HF}$ at about $100^\circ\text{C}$

By

Shiro YOSHIKAWA\*, Nobuatsu WATANABE\* and Masahito ISHII\*

(Received July 31, 1960)

Fluorine generation by fused salt electrolysis of  $\text{KF}\cdot 2\text{HF}$  at medium temperature of about  $100^\circ\text{C}$  was studied from view points of anodic polarization and anode effect. At first, equipment for manufacturing anhydrous HF and a 100 Amp fluorine cell were designed and operated. Various anodic materials (carbons with different grades of graphitization, nickel, C-Cu alloy etc.) were used and the suitable materials for the fluorine generation were selected. Some additional agents ( $\text{LiF}$ ,  $\text{AlF}_3$ ,  $\text{NiF}_2$  etc.) were added to the electrolyte and their effects to anodic polarization were considered from various points. Anodic polarization (or the degree of anode effect) have been proved to have the relation with the wettability of anode by electrolyte. Wettabilities of each electrode were measured by the measurement of sizes, forms and contact angles of bubbles on the anode surface by microphotographic observation. The relation between the wettability and limiting current densities at which anode effect starts, was discussed.

### 1. Manufacturing equipment of Anhydrous Hydrofluoric Acid and 100 Amp. Fluorine Cell.

Firstly, the equipment for manufacturing anhydrous HF consisting of a gaseous HF generator with a rotating rod, a dust chamber, three cooling towers and three reservoirs have been designed. As reagents, concentrated sulfuric acid (98%) and commercial fluorspar (purity 97%) were used, that is, 200 g of fluorspar and sulfuric acid were put into the generator and agitated with the rotating rod. The HF gas generated was first passed through the dust chamber to remove dusts, sulfuric acid, fluorosilicate compounds and water etc. And then it was entered into the first cooling tower, where the other impurities, for example, azeotropes were condensed. In the second cooling tower, the hydrofluoric acid was precooled and in the last tower it was perfectly condensed into the reservoir as liquid state.

Secondly, a 100 Amp fluorine cell has been designed and operated. The inner construction of the fluorine cell is shown in Fig. 2. Several nongraphitized carbon rods (6 cm. in diameter and 50 cm. in length) were used as anodes. The anode

---

\* Department of Industrial Chemistry

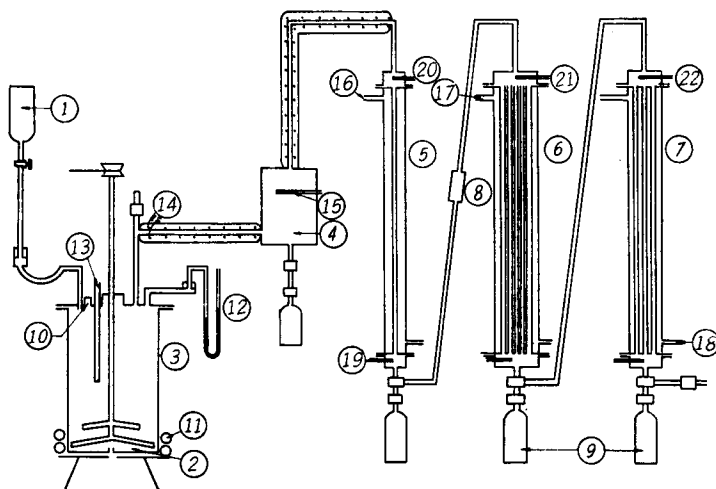
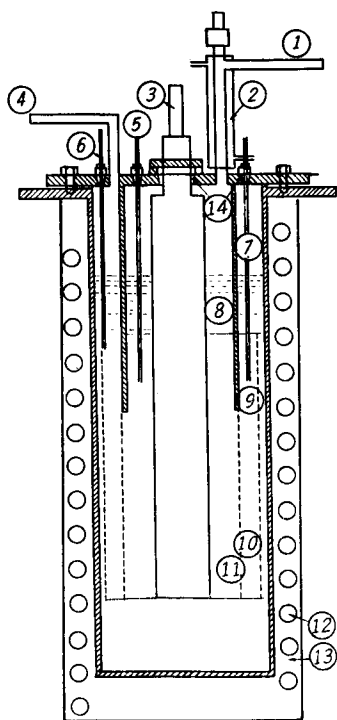


Fig. 1. Anhydrous hydrofluoric acid manufacture equipment.

- ① Conc  $\text{H}_2\text{SO}_4$     ② Fluorspar ( $\text{CaF}_2$ )    ③ Fluoric acid generator
- ④ Dust chamber    ⑤ Cooling tower 1    ⑥ Cooling tower 2
- ⑦ Cooling tower 3    ⑧ Flow meter    ⑨ Receivers
- ⑩ Raw material inlet    ⑪ Heater (gas burner)    ⑫ Manometer
- ⑬ Thermo couple    ⑭ Heater    ⑮ Thermometer
- ⑯ Cooling water outlet    ⑰ Cooling water outlet    ⑱ Cooling liquid inlet ( $-80^\circ\text{C}$ ).
- ⑲    ⑳    ㉑    ㉒ Thermometers



- ① Fluorine outlet pipe
- ② Cooling pipe for condensing HF gas
- ③ Anode
- ④ Hydrogen outlet pipe
- ⑤ Reference electrode
- ⑥ Cathode
- ⑦ Reference electrode
- ⑧ Fused electrolyte ( $\text{KF} \cdot 2\text{HF}$ )
- ⑨ Diaphragm screen
- ⑩ Cathode net
- ⑪ Diaphragm net
- ⑫ Water cooling pipe
- ⑬ Oil jacket

Fig. 2. Fluorine cell.

area is about 7.4 dm<sup>2</sup>. The cathode consists of 8 meshes iron net, which is welded with three iron rods (8 mm.) and insulated from the cell steel cover with Teflon packing. Diaphragm is made of copper and its lower portion is a iron screen. The oil jacket is made of mild steel and has the coiled cooling pipe, through which cooling water passes. The heat medium is liquid paraffine. The capacity of the bath is about 18 L. The cell body which made of mild steel can be charged with 15 L electrolyte. The cell cover carries the hydrogen outlet pipe, hydrofluoric acid feed line, a thermocouple well, fluorine outlet pipe and electrolyte sampling pipe etc. The composition of the electrolyte was from KF·1.86HF to KF·2.2HF. It was often added with 1.0 to 2.0 wt % lithium fluoride into the electrolyte. The cell was operated at 70°C to 110°C. The cell could be operated on a carbon or a nickel anode alone at a low current densities until the water was removed, after which normal operation could be resumed. In the operation of low current densities, cell voltage was kept below 3 volt.

### Manufacture of HF

By operating with different heating temperatures at the generator, different

Table 1. AHF generator operating data.

Rate of dropping of conc H <sub>2</sub> SO <sub>4</sub> . (5 cc/min)	Temperatures of the cooling water in cooling towers.						Reaction temperature of generator (°C)	Temp. of gas (°C)	Press. of generator (mmHg)	Number of gas bubbles uncorrected
	cond. 1		cond. 2		cond. 3					
	inlet	outlet	inlet	outlet	inlet	outlet				
0	29.0	38.0	11.2	12.0	9.5	9.0	120	44	35	14
10	37.0	39.0	11.2	11.9	9.5	9.0		50	80	20
20	54.2	46.1	29.0	19.0	9.7	9.0		56	50	31
30	57.0	52.0	32.8	24.0	14.2	9.0		65	35	10
40	55.0	49.9	33.2	26.2	20.8	9.0		83	80	0
50	56.0	52.8	33.2	27.0	24.8	9.3		90	75	0
60	56.0	53.0	30.9	25.0	24.8	9.7	180	108	77	0
70	51.0	49.0	6.12	23.0	20.0	9.7		113	75	0
80	46.0	42.8	2.01	20.0	17.2	9.7		113	55	0
90	50.0	42.7	29.0	18.0	16.9	9.5		116	10	0
100	44.0	42.0	18.0	17.0	11.2	9.2		121	5	26
110	42.0	41.8	16.0	16.0	10.9	9.0		118	3	30
120	45.0	44.8	15.0	15.0	10.5	9.0		110	3	43
Temp. of cooling water	Ca 42°C		Ca 11°C		Ca 8°C		Dust chamber			
Purity of HF	63.2%		97.2%		99.0%		53.7%			
Yield of AHF	55 g		27 g		163 g		21 g			
Raw material	Fluorspar (CaF <sub>2</sub> ) 600 g 98% conc H <sub>2</sub> SO <sub>4</sub> 650 cc									
Total yield	77.5%									

cooling temperatures and different rates of dropping sulfuric acid, the most profitable conditions were determined. One of these results is given in Table 1.

By this apparatus 200 g. of HF per an hour could be manufactured. The last tower was cooled by  $-80^\circ C$  cooled alcohol, so that the vapour pressure of the condensed anhydrous fluoric acid could be very low.

### Electrolytic generation of fluorine

The electrolyte prepared contains water of 0.6-1.0% (wt) and its water must be removed by the pre-electrolysis. The current-voltage curves in these cases are shown in Fig. 3. At low current densities the potential is too low to discharge  $F^-$  ions to  $F$  molecule, so that water contained must be electrolysed on anode at this low current densities. At 2.4 V  $F^-$  ions may be discharged and fluorocarbon compounds may be also formed by action of the fluorine, accordingly voltage drops from anode to electrolyte increase.

The voltage drops from anode to electrolyte, from electrolyte to cathode and anode probe to cathode probe, as well as the over-all cell voltage are shown as the function of the current densities in Fig. 4 and 5. The voltage drop from anode to electrolyte is seem to be distinctly greater than that from electrolyte to cathode, and the contribution due to the resistance of the electrolyte grows linearly as the current density increases. As shown in Fig. 4 anode effect was suddenly happened at about  $9 A/dm^2$  of current densities. This

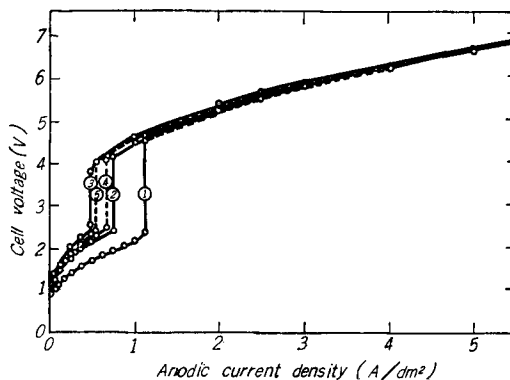


Fig. 3. Current-Voltage curves in the electrolyte containing water.

- ① Before preliminary electrolysis.
- ② After pre-electrolysis for 24 hour at  $0.5 A/dm^2$  of anodic current densities
- ③ After pre-electrolysis for 48 hour at  $0.5 A/dm^2$ .
- ④ In electrolyte added 0.01 wt % water to the electrolyte ③.
- ⑤ After electrolysing the electrolyte ④ for 24 hours at  $0.5 A/dm^2$ .

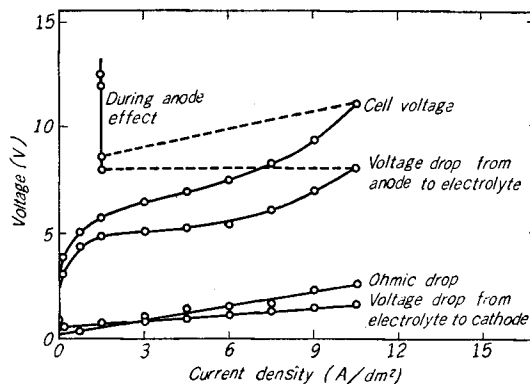


Fig. 4. Current-Voltage curves of the fluorine cell.

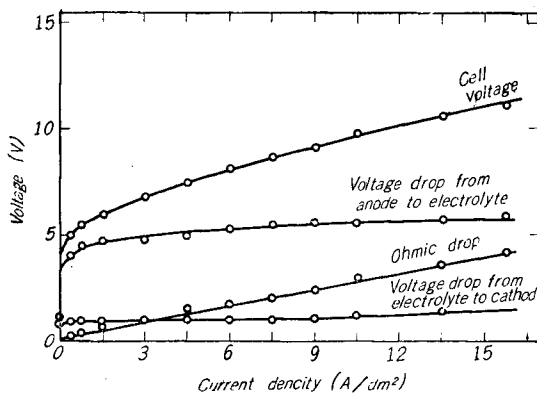


Fig. 5. Current-Voltage curves in electrolyte with LiF (3 wt %).

anodic polarization could be decreased by two our empirical treatments; the addition of 2 wt % lithium fluoride into the electrolyte, and the elimination of the water in electrolyte by means of electrolysis with a nickel anode.

### Conclusion

- 1) By above cooling method, 200 g. of anhydrous fluorine acid could be manufactured per an hour and its purity was over 98%. Cooling power of the towers was decreased by the film formation of fluorocompounds of iron on the wall of the tower.
- 2) From the view points of purity of fluorine gas generated and cell voltage control, water contained in the electrolyte must be removed with nickel anode as perfectly as it can be.
- 3) Addition of lithium fluoride brings good effect to prevent anodic polarization.
- 4) It is the greatest and most difficult problem to prevent explosion by fluorine gas.

### 2. Some influences on the anodic polarization at the electrolytic generation of fluorine

During electrolytic generation of fluorine, one of the most difficult problems is the anodic polarization<sup>1-4</sup>, i.e. anode effect. In the foregoing paragraph, it was reported that in the medium temperature fluorine cell anode effects were observed at 3.5 to 11 A/dm<sup>2</sup> of anodic current densities under various conditions. In this paragraph, further detailed discussions are made for these anodic polarizations including anode effect associated with the anode materials or with the nature of the electrolyte.

**Experimental**

The Fluorine cell of 100 Amp and 1 Amp were used in this study. To observe anodic phenomena in detail, cathode area of 1 Amp cell was by about 10 times larger than that of anode.

**Results**

About 10%, 30%, 50%, 70% and 90% graphitized carbon anodes and nickel anodes were used for the electrolytic generation of fluorine. In Fig. 6, the current-voltage curves are shown for various graphitized carbon anodes, and the limiting current densities at which anode effect occurred are plotted for the grade of graphitization in Fig. 7.

The anode effects were more often observed when higher graphitized carbon anodes were used, especially with anodes of over 50% graphitized carbon the effects occurred easily at even very low current densities. Moreover, the highly graphitized carbon anodes, i.e. graphite anodes swelled up and disintegrated. Anode effect did not occur with nickel anode<sup>5-6</sup>. But it dissolved anodically and formed colloidal nickel fluoride, so it was used for conditioning the electrolyte. As shown in Fig. 8,

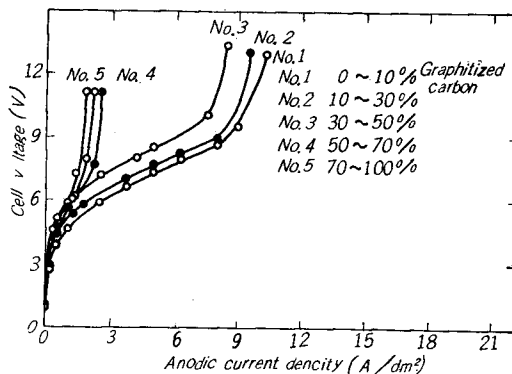


Fig. 6. Current-Voltage curves at different graphitized carbon anodes.

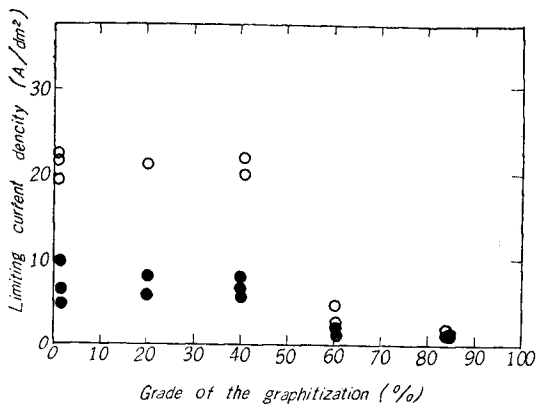


Fig. 7. Limiting current densities with grade of graphitization.

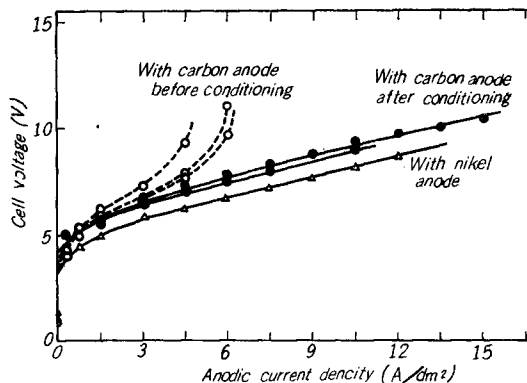


Fig. 8. Effect of conditioning by preliminary electrolysis with nickel anode.

after conditioning anode effect does not occur with carbon anode even at high current densities.

Anodic polarization was influenced not only by the anode materials, but also by the nature of the electrolyte. Lithium fluoride and other fluorides including aluminium fluoride<sup>7-9)</sup> were added to the KF·2HF electrolyte. But most success was obtained with lithium fluoride<sup>10)</sup>, which is slightly soluble in the electrolyte at 100°C. The exact solubility has not yet been ascertained, but it is probable that not much over 1% of lithium fluoride is truly dissolved and possibly even less than this quantity. LiF or AlF<sub>3</sub> was practically added to the bath so that it constitutes about 0.1% to 4.0% (wt).

In Fig. 9, the current-voltage curves are shown for the various percentages of lithium fluoride added.

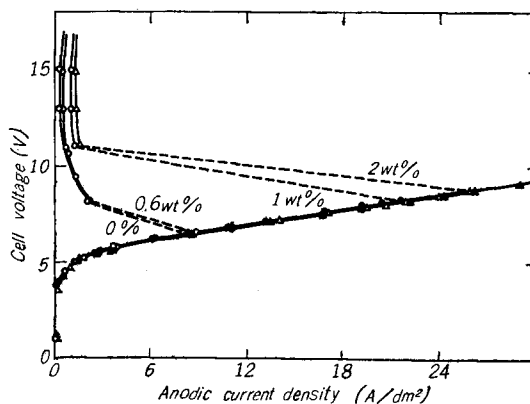


Fig. 9. Current-Voltage curves in electrolyte with LiF.

The relations of these addition and the limiting current densities at which the anode effect occurs are shown in Fig. 10 to Fig. 13. The solubility of lithium fluoride in the conventional electrolyte at 100°C was 0.6 to 0.8% (wt). It was proved by the differential thermal analysis. The addition over 1% resulted the colloidal solution. The effects of these additional agents were remarkable in the colloidal region.

The water contained in the electrolyte does not bring so bad effects<sup>11)</sup>. The relation between the water content and limiting current densities is shown in Fig. 14. The current-voltage curves of the electrolyte containing water were shown in the foregoing paragraph. From authors' experiences, it may be noted here that small quantity of water in electrolyte does not influence much to the anodic polarization, but the HF concentration in the electrolyte does.



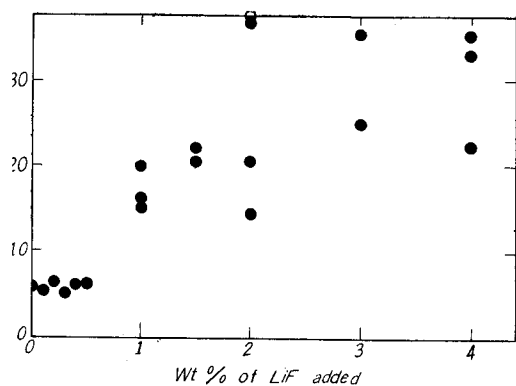


Fig. 10. Limiting current densities in electrolyte with LiF.

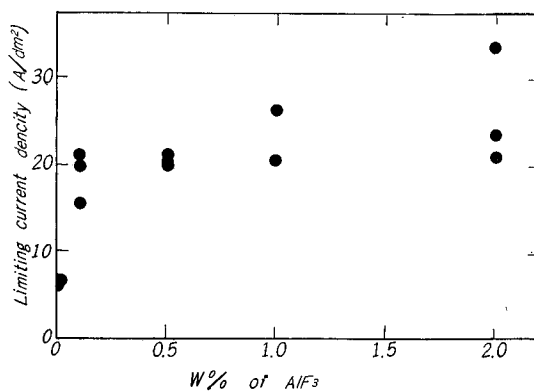


Fig. 11. Limiting current densities in electrolyte with AlF₃.

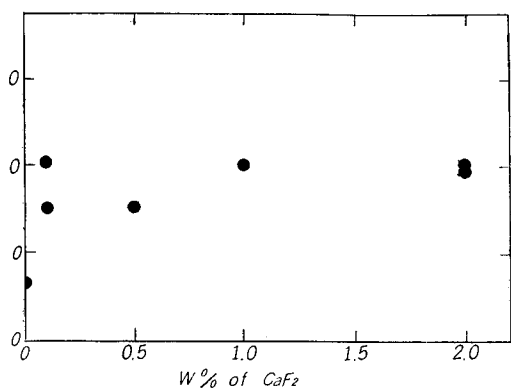


Fig. 12. Limiting current densities in electrolyte with CaF₂.

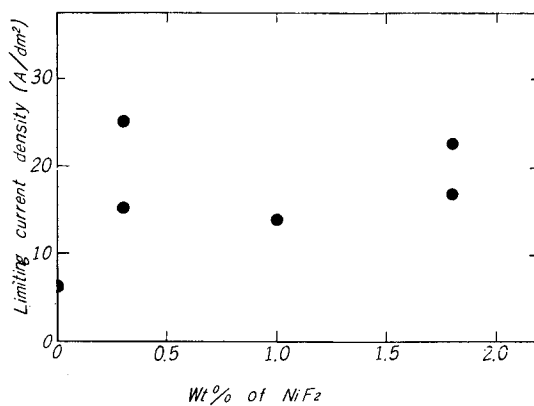


Fig. 13. Limiting current densities in electrolyte with NiF₂.

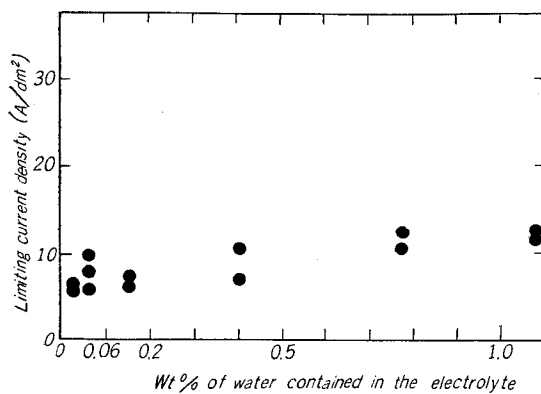


Fig. 14. Limiting current densities in electrolyte containing water.

### Discussion

In the foregoing paragraph, it was reported that the degree of anodic polarization and the anode effect occurrence were influenced by the "Wettability" of the anode by the electrolyte. When the wettability of the anode is small, the greater part of the anode surface is covered by the fluorine gas. The gas bubbles do not leave surface easily and thereby cause anodic polarization. The difference between the graphite anode and nongraphitized carbon anode can be explained as follows: Both the graphite anode and nongraphitized carbon anode are wetted by the electrolyte when they are new, i.e. they are not used as anodes before. But after using as anode, they become nonwetable. These phenomena are more remarkable in the graphite anodes. The decrease of the wettability is occurred due to formation of solid carbon fluoride film on the anode surface by the reaction of fluorine.

As these carbon fluoride films are pointed by Ruff<sup>12)</sup> and Rüdorff<sup>13-16)</sup>, or as shown in polyfluoroethylene resin, they have a tendency to decrease the wettability. At graphite anodes the fluorocarbon film is more easily formed than at carbon anodes. This is shown in Table 2, where in case of A anode material was exposed to fluorine stream for 26 hrs. and B for 30 minuts. At graphite anodes, anode effects occurred more easily. The colloidal nickel fluoride formed during conditioning the electrolyte was also found to retard the formation of fluorocarbon compounds on the anode surface. The colloidal solution of lithium fluoride or aluminum fluoride does not condition the electrolyte, but seems to stop the formation of fluorocarbon film on the anode surface.

Table 2. Reactivity with fluorine.

Anode material	A	B
	Increase of weight.	Increase of weight.
Graphite	6 wt %	0.13 wt %
Carbon	0.28 wt %	0.01 wt %

### Conclusion

- 1) From the view-point of anodic polarization, low grade of graphitization hard carbon is most profitable. Fluoro-compounds which decrease wettability of anode are more easily formed at graphite than at non-graphitized carbon anode.
- 2) Effect of conditioning by electrolysis with nickel anode is due to the formation of colloidal nickel fluoride which was anodically dissolved.
- 3) Addition of lithium fluoride and Aluminium fluoride etc. brings good effect to prevent anodic polarization. It is found that the effects of these additional agents were remarkable in the colloidal region.

### 3. Relations between the wettability of anode and the anodic polarization in the electrolytic generation of fluorine

In the foregoing paragraphs 1.2, it was reported that anodic polarization and anode effect were influenced by the wettability of the anode by the electrolyte. In this paragraph, "Wettability" is more quantitatively measured by observation of forms and sizes of the gas bubbles on the anode surface. They are changed by the mutual effects of the interfacial tension of the electrolyte, anode materials, current density and anodic potential etc., and the wettability changes could be ascertained by measuring them.

**Theory on "Wettability".** When an electrode is inserted in a solution, adsorption of liquid takes place on electrode surface. If the fraction of electrode surface on which liquid adsorbed is  $\alpha$  ( $0 \leq \alpha \leq 1$ ), then, the fraction  $(1-\alpha)$  is covered by gas molecule. "Wetting of solid by liquid" means that the liquid adsorbs on the solid in place of the gas which has already adsorbed. The work done for this exchange is equal to the change of the surface energies of the liquid ( $\gamma_e$ ), solid ( $\gamma_s$ ) and liquid-solid interface ( $\gamma_i$ ), that is,  $Wa = \gamma_s + \gamma_e - \gamma_i$ . According to the Young's formula;  $Wa = \gamma_e(1 + \cos \theta)$ , where  $\theta$  is the contact angle between the solid and the liquid and from Doss's equation<sup>17)</sup>;  $Wa = 2\alpha\gamma_e$ , the relation between  $\alpha$  and  $\theta$  can be easily obtained by the equation;  $\alpha = (1 + \cos \theta)/2$ . Therefore, by measuring the contact angle of the bubbles on the anode surface, fraction  $(1-\alpha)$  of the surface which is covered by gas molecules can be estimated. The fraction  $(1-\alpha)$  has insulating effect due to formation of polylayers of gas molecules. In the liquid i.e. in the electrolyte, due to mutual relations of the interfacial tensions, the gas layers on  $(1-\alpha)$  are always poly-layers and insulate direct current. If the contact angle  $\theta$  is larger, the fraction  $\alpha$  will be smaller and the greater part of the anode surface will be covered by nonconducting gas layers. When anode effect occurs, the contact angle  $\theta$  will be  $180^\circ$  ( $\alpha=0$ ,  $Wa=0$ ), that is, the anode surface will be completely covered with the nonconducting gas molecules. The degree of the anodic polarization and the limiting current densities at which anode effect occurs depend on the rate of the desorption of gas bubbles from the electrode, and it is likely to be the function of wettability of the electrode. The more wettable is the electrode, the easier to desorb the gas from it. Therefore, by measuring the contact angle  $\theta$ , the rate of desorption of gas from the electrode can be approximately estimated<sup>18,19)</sup>.

The fluorine ions discharge on the electrode and become fluorine molecules, which adsorb on the electrode with the rate of  $V_1$ , and these adsorbed fluorine gases leave from it with the rate of  $V_2$ . If the rate of the adsorption  $V_1$  is

smaller than the rate of desorption  $V_2$ , normal conditions of electrolysis are obtained. While again if the current densities are increased,  $V_1$  becomes larger than  $V_2$ , the produced gases will accumulate on the electrode, consequently anode effect will occur. The current density at which anode effect just starts is termed "limiting current density" when  $V_1$  comes up to  $V_2$  at par or greater i.e.  $V_1 \geq V_2$ . As the rate of desorption is influenced by the wettability, anode effect will easily occur with less wettable electrode.

The Wettability of the electrode is influenced by the anode material, surface tension of the electrolyte, current densities, anodic potentials, and the compounds which are formed during electrolysis on the electrode surface (for example, solid fluorocarbon compounds). In these points of view, the wettabilities of electrodes are measured by microphotographic observation of the gas bubbles on electrode surface. In the light of above observations the relations between wettability and anodic polarization are discussed below.

### Experimental

For microphotographic records of gas bubbles on the electrode surface, a special transparent cell was devised. It was put into a box which was made of fire bricks and was illuminated from behind. The images of the gas bubbles on the electrode were magnified (15 times) by a lens and caught by a camera. The cell ( $10 \times 8 \times 2.5$  cm) was made of polyfluoroethylene resin. These apparatus are shown in Fig. 15 and Fig. 16.

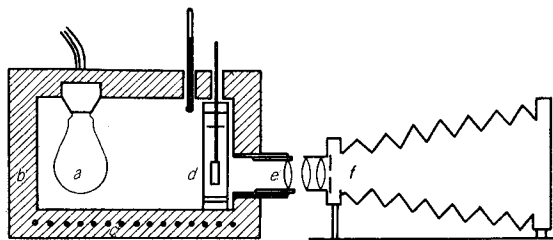


Fig. 15. Arrangement for microphotographical measurement of the gas bubbles.

- (a) 100W lamp.
- (b) Box which is made of fire bricks.
- (c) Heater.
- (d) Transparent cell.
- (e) Lens.
- (f) Camera.

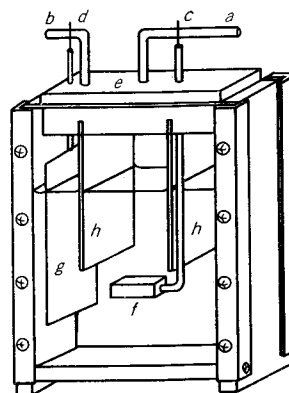


Fig. 16. Transparent fluorine cell.

- (a) Fluorine outlet pipe.
- (b) Hydrogen outlet pipe.
- (c) Anode lead wire.
- (d) Cathode lead wire.
- (e) Teflon cell cover.
- (f) Anode.
- (g) Cathode (nickel).
- (h) Diaphragm (Teflon).

### Results and discussion

Forms and sizes of the gas bubbles in fused salt electrolysis are much different from those in aqueous solution. The bubbles of fluorine gas which are generated in the fused electrolyte;  $KF \cdot 2HF$  at about  $100^\circ C$  are shown in Photo. 1. Chlorine

gas bubbles in electrolysis of sodium chloride solution are shown in Photo. 2 and 3. Photo. 4 and 5 present the gas bubbles in  $KF \cdot 3HF$  and  $KF \cdot 2HF$  respectively. The bubbles of the chlorine gas are very small (below 0.1 mm in diameter). But the bubbles of the fluorine gas are as large 10 mm in diameter and their contact angles are greater than  $150^\circ$ . Therefore, in the fused electrolyte the wettability is very low compared to that in aqueous solution. This fundamental difference in the wettability explains the cause of the anode effect and this characteristic phenomenon was observed only in the fused salt

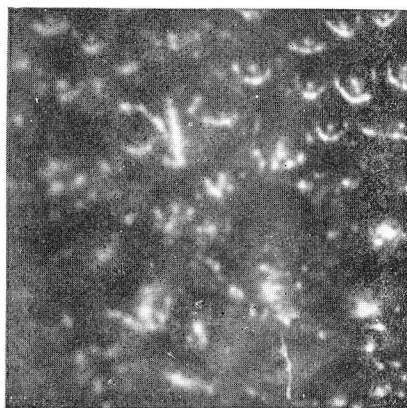


Photo. 1. ( $\times 1.5$ )

Fluorine gas bubbles on carbon anode at the anodic current densities of  $0.5 A/dm^2$  in fused electrolyte ( $KF \cdot 2HF$ ).

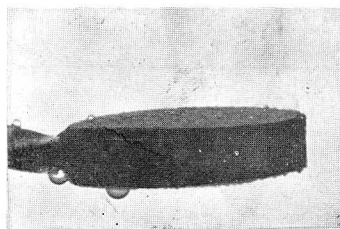


Photo. 2.

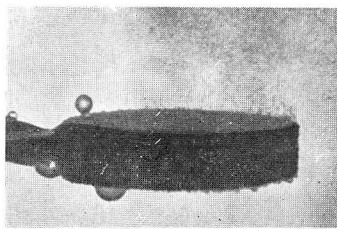


Photo. 3.

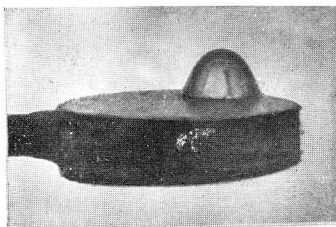


Photo. 4.

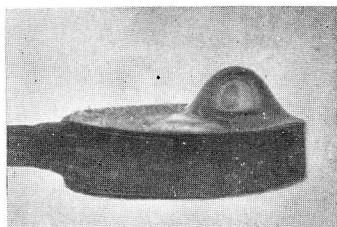


Photo. 5.

Bubbles in the various electrolyte on the same electrode. ( $\times 1.5$ )

Photo. 2.  $NaCl$  solution at  $25^\circ C$ ,  $D_A = 0.5 A/dm^2$ .

Photo. 3.  $NaCl$  solution at  $25^\circ C$ ,  $D_A = 1.0 A/dm^2$ .

Photo. 4.  $KF \cdot 3.2HF$  at  $80^\circ C$ ,  $D_A = 1.0 A/dm^2$ .

Photo. 5.  $KF \cdot 2.0HF$  at  $90^\circ C$ ,  $D_A = 1.0 A/dm^2$ .

electrolysis. At close study of Photo. 4 and Photo. 5, it reveals that the lower conc. of HF in the electrolyte produced large gas bubbles and consequently the anode was less wettable. For this reason the anode effects and anodic polarizations are observed more frequently at the lower HF concentration. Anode effect is not observed during the electrolysis with the metallic anode. The bubbles of fluorine gas on the nickel anode are shown in Photo. 6a and Photo. 7a. The bubbles are as small as those of chlorine gas on electrolysis of sodium chloride solution. Their contact angles are also near to zero. Therefore, the wettability of the nickel anode by the fused electrolyte of  $\text{KF}\cdot 2\text{HF}$  is very high. In the graphite and nongraphitized carbon anodes, the greater is the degree of graphitization, lesser is the wettability and thereby the anode effects occurred more easily even at low current densities. As reported in the earlier paper, the solid film of the fluorocarbon is more easily formed at the graphite anode. Accordingly, the decrease of the wettability of graphite anode is greater than that of nongraphitized carbon anode. The bubbles of hydrogen gas on the cathode of same material of anode are shown in Photo. 8b and Photo. 9b. Sizes of the hydrogen bubbles are very small compared to that of fluorine bubbles and their contact angles are also nearly to zero. That means, the cathode is very much wettable even in the fused electrolyte. And the fluorocarbon compounds which decrease the wettability of electrode do not exist at the cathodes. It has been reported

already that fresh anodes of graphite and nongraphitized carbon are wettable, while they became nonwettable after use. The change in cell voltage with time during the electrolysis with a fresh electrode at constant anodic current densities of  $0.5 \text{ A/dm}^2$  is shown in Fig. 17. At various points in the curve, photographs of the gas bubbles were taken and they are shown in Photo. 10 to Photo. 15. As the cell voltage increases, the

sizes and contact angles of the bubbles become larger and wettabilities decrease. It was already discussed that these phenomena were owed to the formation of the fluorocarbon compounds at the electrode surface. Relation between the

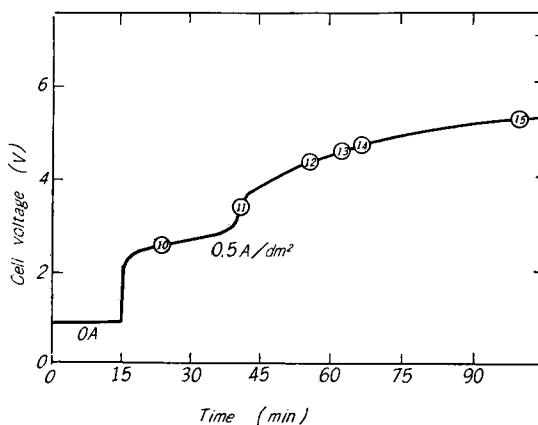


Fig. 17. Cell voltage with time at constant current densities of  $0.5 \text{ A/dm}^2$ .

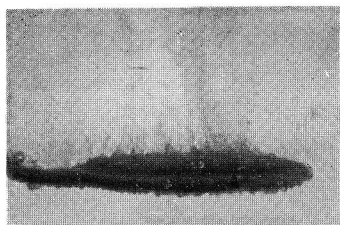


Photo. 6a.

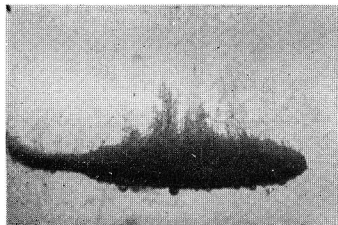


Photo. 7a.

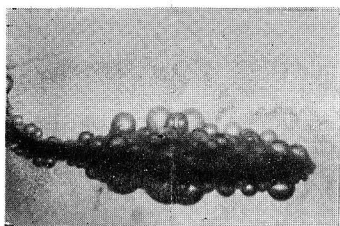


Photo. 6b.

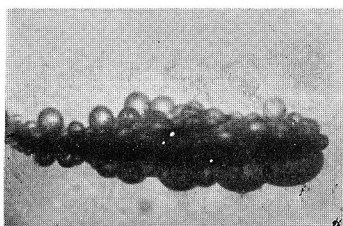


Photo. 7b.

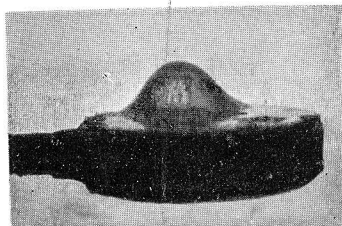


Photo. 8a.

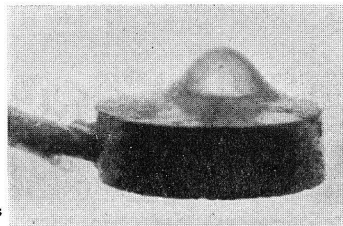


Photo. 9a.

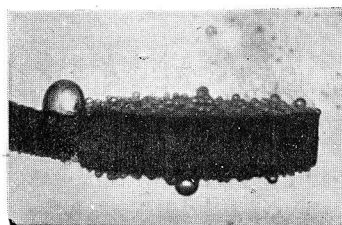


Photo. 8b.

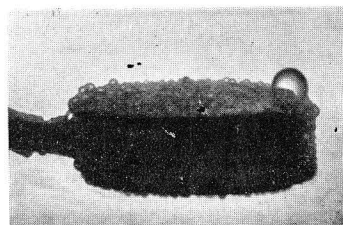


Photo. 9b.

Bubbles on the various electrode in fused  $KF \cdot 2HF$ . ( $\times 1.5$ )

- Photo. 6a. Fluorine bubbles on the nickel anode ( $0.5 A/dm^2$ ).
- 6b. Hydrogen bubbles on the nickel cathode ( $0.5 A/dm^2$ ).
- Photo. 7a. Fluorine bubbles on the nickel anode ( $1.0 A/dm^2$ ).
- 7b. Hydrogen bubbles on the nickel cathode ( $1.0 A/dm^2$ ).
- Photo. 8a. Fluorine bubble on the carbon anode ( $1.0 A/dm^2$ ).
- 8b. Hydrogen bubbles on the carbon cathode ( $1.0 A/dm^2$ ).
- Photo. 9a. Fluorine bubble on the graphite anode ( $1.0 A/dm^2$ ).
- 9b. Hydrogen bubbles on the graphite cathode ( $1.0 A/dm^2$ ).

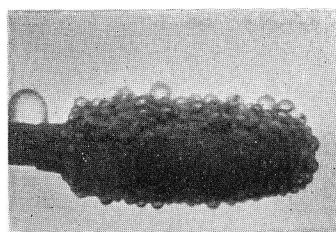


Photo. 10.

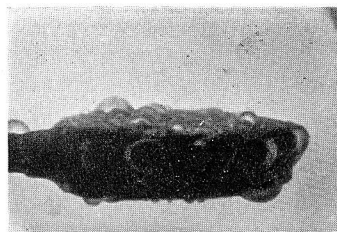


Photo. 11.

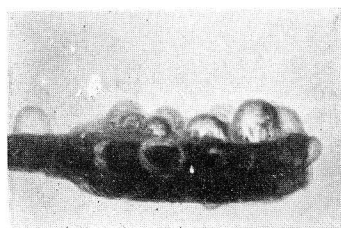


Photo. 12.

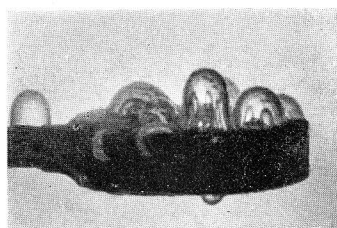


Photo. 13.

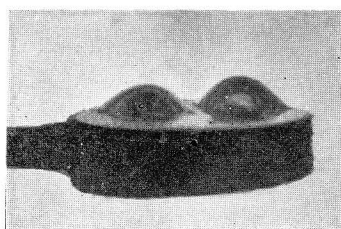


Photo. 14.

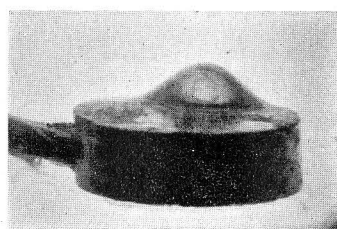


Photo. 15.

Changes of bubble sizes and forms with time on the new electrode at the constant current densities of  $0.5 \text{ A/dm}^2$ . ( $\times 1.5$ )

Table 3. Wettability and Limiting current density.

Anode material	electrolyte	gas generated	Surface tension of electrolyte ( $\gamma_e$ )	Contact angle ( $\theta$ )	Wettability of electrode $Wa = \gamma_e(1 + \cos \theta)$	Size of gas bubble $\text{cm}^3$	Limiting current density. $\text{A/dm}^2$
Nickel	KF·2HF	F <sub>2</sub>	100	$\approx 0^\circ$	200	$1 \times 10^{-7}$	$\approx \infty$
Carbon	NaCl aqueous solution	Cl <sub>2</sub>	70	$\approx 0^\circ$	140	$3 \times 10^{-7}$	$\approx \infty$
Carbon (Fresh)	KF·2HF	F <sub>2</sub>	100	30-60	180-150	$1 \times 10^{-4}$	—
Carbon	KF·2HF	H <sub>2</sub>	100	10-40	198-164	$1 \times 10^{-4}$	—
Graphite	KF·2HF	H <sub>2</sub>	100	10-40	198-164	$1 \times 10^{-4}$	—
Nickel	KF·2HF	H <sub>2</sub>	100	30-90	180-100	$4 \times 10^{-3}$	—
Carbon (old)	KF·3HF	F <sub>2</sub>	75	160	17	0.095	6-8
Carbon (old)	KF·2HF	F <sub>2</sub>	100	150-170	13-15	0.1-0.3	5-6
Graphite (old)	KF·2HF	F <sub>2</sub>	100	160-170	13-14	0.35	2-3



wettability and the limiting current densities is tabulated in Table 3. When the anodic potential changes, the interfacial tensions must be changed as shown in the electrocapillary curves. In Photo. 16 to Photo. 20, the gas bubbles at different current densities are shown. In Photo. 21 to Photo. 25, the bubbles on the vertical electrodes are shown. The forms and sizes of the gas bubbles immediately before the occurrence of anode effects are shown in Photo. 20 and Photo. 23. At the time the electrodes are entirely covered with gas films. In Photo. 24 the forms of gas bubble during anode effect are shown. From these Photographs it appears that at the time of anode effect occurrence the electrode was completely covered the gas films. Further generation of gas could not be recognized. The larger bubbles on the electrode annex the smaller bubbles which are produced

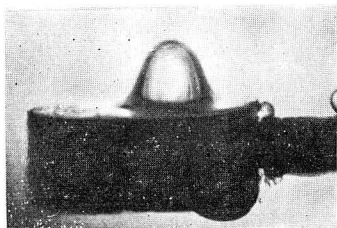


Photo. 16.

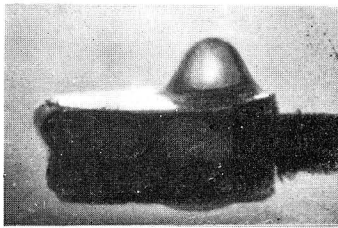


Photo. 17.

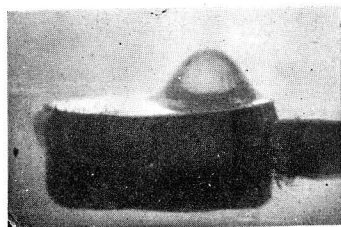


Photo. 18.

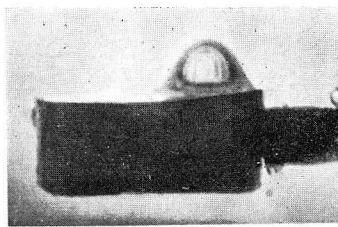


Photo. 19.

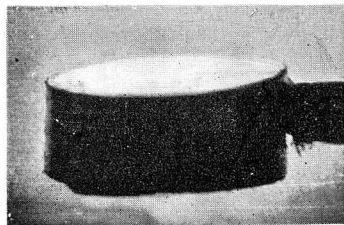


Photo. 20.

Changes of bubble forms with the current density ( $\times 1.5$ )

- Photo. 16. Fluorine bubble on the carbon anode at  $0.5 \text{ A/dm}^2$ .
- Photo. 17. At  $1.0 \text{ A/dm}^2$ .
- Photo. 18. At  $3.0 \text{ A/dm}^2$ .
- Photo. 19. At  $5.0 \text{ A/dm}^2$ .
- Photo. 20. At  $6.2 \text{ A/dm}^2$  immediately before anode effect occurrence.

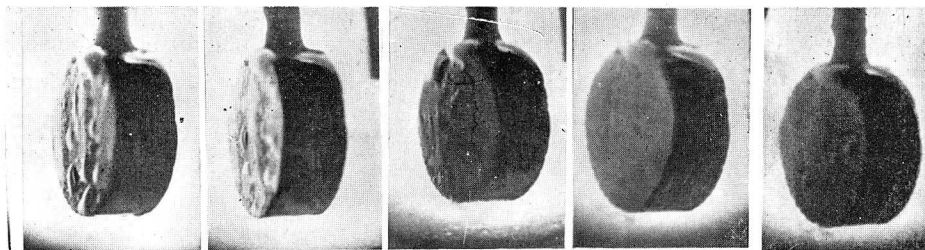


Photo. 21.

Photo. 22.

Photo. 23.

Photo. 24.

Photo. 25.

Changes of bubble forms with the current density ( $\times 1.0$ )

Photo. 21. Fluorine gas bubbles on the hard carbon anode at  $0.5 \text{ A/dm}^2$ .

Photo. 22.  $4.0 \text{ A/dm}^2$ .

Photo. 23.  $6.4 \text{ A/dm}^2$  immediately before anode effect occurrence.

Photo. 24. During anode effect occurrence.

Photo. 25.  $2.0 \text{ A/dm}^2$  32 minutes after cutting the direct current.

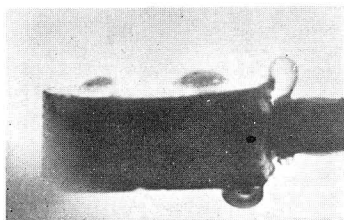


Photo. 26.

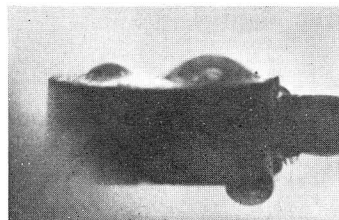


Photo. 27.

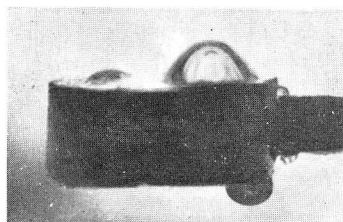


Photo. 28.

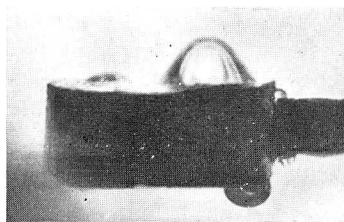


Photo. 29.

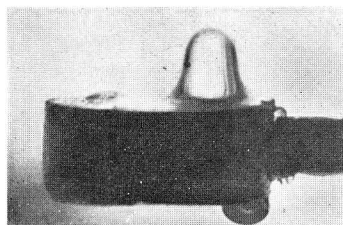


Photo. 30.

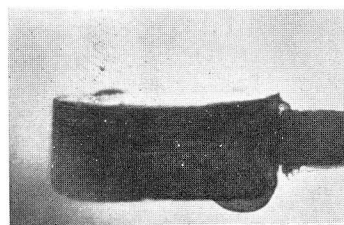


Photo. 31.

Growth of fluorine bubbles ( $D_A=0.5 \text{ A/dm}^2$ ) ( $\times 1.5$ )

Photo. 26. 10 second after the moment of delivrence of the bubble.

Photo. 27. 20 second.

Photo. 28. 31 second.

Photo. 29. 33 second.

Photo. 30. 35 second immediately before the deriverence of the bubble.

Photo. 31. 37 second immediately after the deriverence of the bubble.

at the active section of the electrode and become larger. The section where the small gas bubbles are produced is wetted and the section where the large gas bubbles adsorb is inactive dry place. The grown large bubbles leave only from the inactive nonwetted electrode surface. The mechanism of the growth of the gas bubbles are shown in Photo. 26 to Photo. 31.

### Conclusion

- 1) Anodic polarization has relation with wettability and anodic polarization is greater at nonwetttable anode. Metallic anodes are wetted by the fused electrolyte (KF·2HF), accordingly anode effect can not occur.
- 2) Carbon and graphite anode is not wetted by the fused electrolyte (KF·2HF) because of the formation of fluorocompounds, which decrease wettability of anode.
- 3) Anode effect is occurred by nonconducting gas film which covers perfectly anode surface.
- 4) Sizes of the fluorine gas bubbles on the carbon and graphite electrode are very large, (over 10 mm in diameter) and their contact angles are beyond 150°, i.e. they have forms like lens.

### Literature

- 1) P. Lebeau and A. Damiens; *Compt. Rend.*, **181**, 917 (1925).
- 2) C. H. Cady; *J. A. C. S.*, **57**, 246 (1935).
- 3) J. T. Pinkston; *Ind. Eng. Chem.*, **39**, 255 (1947).
- 4) G. H. Cady and C. A. Carlson; *Ind. Eng. Chem.*, **34**, 443 (1942).
- 5) P. M. Lebeau and A. Damins; *G. P.* 4767327-12-1926.
- 6) R. C. Dowing, A. F. Benning et al.; *Ind. Eng. Chem.*, **39**, 259 (1947).
- 7) W. C. Shumb, R. C. Young et al.; *ibid.*, **39**, 244 (1947).
- 8) John Pinkston et al.; *ibid.*, **39**, 255 (1947).
- 9) Vavalides et al.; *ibid.*, **50**, 178 (1958).
- 10) A. J. Rudge; *Chem. and Ind.*, 247 (1949).
- 11) Fredenhagen and Krefft; *Zeit. Electrochem.*, **35**, 670 (1929).
- 12) O. Ruff and O. Bretschneider; *Z. Anorg. Chem.*, **217**, 1 (1934).
- 13) W. Rüdorff and G. Rüdorff; *Ber.*, **80**, 413 (1947).
- 14) W. Rüdorff and G. Rüdorff; *ibid.*, **80**, 417 (1947).
- 15) W. Rüdorff; *Z. Anorg. Chem.*, **254**, 319 (1947).
- 16) W. Rüdorff et al.; *ibid.*, **256**, 125 (1948).
- 17) K. S. Doss and B. S. Rao; *Proc. Indian. Acad. Sci.*, **7A**, 117, (1938).
- 18) B. Kabanov and A. Frumkin; *Z. physik. Chem.*, **A165**, 433 (1933).
- 19) B. Kabanov and A. Frumkin; *ibid.*, **A166**, 316 (1933).